N86-17847

GaAsP ON GaP TOP SOLAR CELLS*

James B. McNeely, Gerald H. Negley, and Allen M. Barnett
Astropower Division
Astrosystems, Inc.
Newark, Delaware

GaAsP on GaP top solar cells as an attachment to silicon bottom solar cells are being developed. The GaAsP on GaP system offers several advantages for this top solar cell. The most important is that the gallium phosphide substrate provides a rugged, transparent mechanical substrate which does not have to be removed or thinned during processing. Additional advantages are that 1) gallium phosphide is more oxidation resistant than the III-V aluminum compounds, 2) a range of energy band gaps higher than 1.75 eV is readily available for system efficiency optimization, 3) reliable ohmic contact technology is available from the light-emitting diode industry, and 4) the system readily lends itself to graded band gap structures for additional increases in efficiency.

INTRODUCTION

The optimum band gap for a top solar cell on a silicon bottom cell (1.1 eV) lies between 1.75 and 2.07 eV [1]. Top solar cell layer compositions corresponding to band gaps of 1.75 eV or higher are being investigated to determine the optimum band gap as a function of real device and system performance. For example, the potential gain in minority carrier diffusion lengths at 2.1 eV, due to a reduced lattice mismatch, may net a higher system efficiency.

GaAsP TOP SOLAR CELL DESIGN

The GaAsP on GaP top solar cell design is based on a model used to calculate theoretical maximum efficiencies of tandem solar cell systems. The model that is being used follows that described by Fan [1].

Assuming unity quantum efficiency and no losses, the model predicts a maximum tandem solar cell efficiency of 34.8% for the AMO spectrum at a one sun insolation. This optimum performance is based on a four-terminal configuration. The top solar cell has an energy gap of 1.97 eV and the calculated performance for both ideal solar cells is shown in Table I.

*Partial support has been provided by the Air Force AeroPropulsion Laboratory under Contract No. F33615-84-C-2486.

Table I.

Ideal Tandem Solar Cell Model - AMO
(Bottom Cell - Silicon)

Gap (eV)	Jsc (mA/cm^2)	Voc (volts)	FF	Efficiency (%)
1.97	20.75	1.50	0.91	21.1
1.12	32.68	0.67	0.84	13.7
				34.8

The actual anticipated efficiencies can be modeled by considering losses [2]. The one sun losses are tabulated below in Table II.

Table II.

Tandem Solar Cell Model with Losses:

- Optical and recombination losses which reduce Jsc as follows:

Loss	
Top surface reflection -	2.6%
Grid Shading - top cell	4.0%
Absorption losses - top cell	2.0%
Absorption losses - bottom cell	9.0%
Recombination losses - top & bottom cell	6.2%
Bottom grid shading loss - bottom cell only	4.0%
Reflection loss - bottom cell only	1.0%

- Electrical losses, which reduce fill factor:

Loss	
Series resistance losses - both solar cells	2.0%

Gap (eV)	Jsc (mA/cm^2)	Voc (volts)	FF	Efficiency (%)
1.97	17.8	1.50	0.89	17.6
1.12	24.8	0.67	0.82	10.1
				27.7

Another useful case is based on an energy gap larger than the optimum of 1.97 eV. For example, at 2.07 eV, the arsenic concentration can be reduced from x = 0.54 to x = .40, leading to a reduced lattice mismatch of 1.5% from 2.0%. The energy conversion efficiency reduction from the optimum may be offset by longer actual diffusion lengths based on reduced lattice mismatch. This design clearly merits further examination. The analysis of this design (2.07 eV) leads to a predicted tandem solar cell efficiency of 34.5% which is similar to that predicted by the optimized design at 1.97 eV.

Finally, the GaAsP on GaP system lends itself to graded energy gaps on both sides of the junction. It has been shown that this can lead to as much as an 11% increase in energy conversion efficiency

[3]. This graded energy gap design will be studied to maximize system conversion efficiency.

A range of energy gaps between 1.75 eV and 2.07 eV for the top solar cell junctions is being explored during this program.

DEVICE PREPARATION

The solar cell structure is being grown using liquid phase epitaxial growth. The advantages of liquid phase epitaxy are excellent transport properties, minimum contamination, uniform thickness control, and reductions in point defects and dislocations. Liquid phase epitaxial growth has, in general, demonstrated devices that are superior in performance to those grown by the other methods [4,5]. These superior performance devices include light emitting diodes, semiconductor lasers, magnetic garnet bubble memories and GaAs solar cells. The improved performance of liquid phase epitaxial, LPE, devices when compared to vapor phase or diffused devices can be attributed to the exact stoichiometry control, longer diffusion lengths, fewer deep levels and the tendency of impurities to segregate to the liquid rather than the solid.

Ideally, one would like to grow epitaxial layers on lattice-matched substrates. While this is not possible with the GaAsP on GaP devices, we have demonstrated lattice-mismatched liquid phase epitaxial growth of GaAsP on gallium phosphide substrates. Recently multiple graded layers of GaAsP on GaP with a composition of $GaAs_{.68}P_{.32}$ corresponding to a band gap of 1.81 eV have been grown with smooth morphologies in our laboratories. The overall degree of lattice mismatch between $GaAs_{.68}P_{.32}$ (a_o = 5.5886) and GaP (a_o = 5.45117) is 2.52%. This growth was accomplished by three individual grading layers each accommodating 1.86%, 0.33%, and 0.33% of the lattice mismatch, respectively. Grading was readily accomplished by melt depletion. Moon and co-workers [6] have independently shown feasibility of liquid phase epitaxial grading to obtain smooth layers that are mismatched relative to the substrate for the GaAsP and other ternary and quaternary systems. The $GaAs_{1-}P_x$ graded layer from Moon's work shows uniform compositional grading for GaAsP system and smooth growth morphology for a $GaAs_{0.6}P_{0.4}$ layer on which corresponds to a 2.22% lattice mismatch in a single layer.

These results are indeed encouraging. The optical transmission of the three GaAsP layers grown by us are shown in Figure 1.

Mismatch dislocations result from compositional discontinuities and from composition variations that are too large for the layers to accommodate the mismatch within the graded layer. A method of reducing misfit dislocations to zero has been described [7]. This method uses a two-stage top layer growth from similar melts to achieve zero misfit dislocation growth. Misfit dislocations are pinned at the termination of the first layer growth, making extension of the misfit dislocation in the second homo-epitaxy layer difficult.

Characterization of these layers is by optical transmission, optical microscopy, spectral response, scanning electron microscopy,

EDAX and misfit dislocation decoration and analysis. Minority carrier diffusion length will be optimized based on variations in growth parameters and compositions.

Solution growth of multi-layer structures of GaAs-GaP will be performed using the slider method developed for liquid phase epitaxial growth [8]. The slider apparatus serves as a substrate holder and melt container for the growth solutions. Advantages of the slider apparatus over other techniques, such as dipping, are 1) the substrate wafer can be brought in and out of contact with the melts, 2) several melts can be used in sequence, 3) growth is restricted to a single side of the wafer, 4) substrate-solution contact is from the bottom of the melt where there are no floating oxides or other contaminants, 5) excess solution can be wiped off the wafer by the slider action of the boat, and 6) thermal equilibrating and temperature profiling are greatly facilitated. The graphite slide apparatus fits into a cooling or temperature gradient furnace, as appropriate. The furnace zones can be controlled to better than $1^{o}C$. We use a furnace atmosphere based on a high purity mixture of hydrogen or 15% hydrogen and 85% nitrogen, which is continuously sweeping the furnace and slider apparatus during the furnace operation.

A feature of the slider boat apparatus particular to this program is the grading of the width of the growth wells shown in Figure 2. This graded well width design permits individual access to each of the grown layers after the substrate is removed from the boat.

Based on thermodynamic considerations, the preferred solvent for the p-layer is gallium, and for the n-layer, gallium or tin. Both of these materials are available commercially with purities in excess of 99.9999%. Both p-type and n-type single crystal gallium phosphide are available commercially with various dopants and doping levels, consistent with device design considerations. Melts are composed of about 10 grams of solvent and appropriate amounts of GaP and GaAs. Growth is accomplished by placing the GaP substrates under the first melt to grow a transition layer of $GaAs_xP_{1-x}$ by controlling the temperature level, cooling rate, and time of exposure, and continuing, in turn, to each melt shown in the growth apparatus in Figure 2 until all requisite layers are grown.

Phase equilibria data have been determined for both the gallium and tin solvent systems.

The specific multi-layer structure being grown is based on our demonstrated growth to date tailored to have a uniformly graded structure. The structure is shown in figure 3 and is composed of four basic layers. The first three layers are graded in composition in a controlled manner either as finite composition steps, or as continuous compositional variations shown in Figure 4. The continuous compositional variations are achieved by melt depletion. The fourth layer is a thin cap layer. These layers, the method for preparation, and methodology for optimization are described in the next four paragraphs.

This structure can be produced readily in the LPE apparatus with equal facility for either n on p or p on n structures. Either zinc or

magnesium will be used in the top $GaAs_xP_{1-x}$ layer to form the p/n junction, and tellurium will be used to form the n/p junction. The salient feature of this design is that the band gap of top of each layer is 2.07 eV, 1.95 eV, and 1.75 eV band gaps. Growth may be truncated at individual layers of interest, and comparison of otherwise equivalent material may be made with only the stated variations in band gap. This permits experimental optimization of band gap during preparation of the structure. The added benefit of this structure is that each successive layer has only about 0.6% lattice mismatch, and at no point in the top two graded layers does the structure grade more than 2 mole % GaAs per micron of growth. This allows the top layers to be reasonably thin and insures their equivalency for the optimization experiments.

This graded layer structure does not represent an excessive number of layers even with intermediate layers. Our current boat design operates with up to nine melts.

The compositional variation with layer thickness is shown in Figure 4. For the top two layers, the curvature is very slight and the compositional variation is nearly a linear function. Indeed, the differential or slope of composition with respect to thickness increases only slightly as the final compositions with each layer are approached. Other variables, growth time, temperature level, growth rate and melt size, can be varied based on detailed comparison of the experimental results. Initial and final temperature and melt compositions establish the grown layer composition. Melt size and wafer area determine layer thickness. Cooling rate and growth time are dependent on each other since initial and final temperatures are fixed for a given growth situation. For example, slowing the actual growth rate can be done to improve crystal morphology, leading to increased growth time. Intermediate dislocation blocking layers are also planned after the first layer and the second layer are grown if necessary.

The cap layer is a thin grown layer. The cap serves to reduce surface recombination and can also serve as a source of dopant for a diffused junction [9]. This layer will be either GaP or $Ga_yAl_{1-y}As_xP_{1-x}$ material with initial experiments using gallium phosphide. $Ga_yAl_{1-y}As_xP_{1-x}$ will be used if interface dislocations due to GaP lattice mismatch prove to be a problem. Gallium phosphide has a high oxidation resistance, and it has been studied extensively in terms of metallic ohmic contacts. The cap layer will be thin enough so that it minimizes the effect on the crystal structure in the underlying active region. The cap layer is basically a conducting layer and serves to reduce the surface recombination velocity of the adjacent layer; it is probably not necessary that this layer possess the crystalline perfection of the preceding layers. Therefore, a interfacial compositional discontinuity may be tolerated between the cap layer and the top active layer. However, aluminum additions to the structure will be used, if needed, to optimize lattice matching for the cap layer. The cap layer may be grown from a tin solution for n-type layers, or from gallium for p-type layers.

CONTACTS

With the grown multi-layer wide band gap structure described above, the next task is to form ohmic contacts on the top and bottom surfaces of the wafer. No thinning prior to contact formation is required with this solar cell design because the gallium phosphide substrate is transparent to photons less energetic than the band gap of the active junction of the top cell. The structure is, in fact, quite sound mechanically and, therefore, is expected to have low breakage and high fabrication yields during subsequent processing.

The n-type contact consists of thermally evaporated Au/Ni or Au/Ge/Ni on a clean wafer surface. Surfaces are etched prior to evaporation using 1:1 HCl-H_2O and are rinsed thoroughly in 18-meg ohm deionized water, dried, and placed immediately in the evaporator. Evaporation is done using tungsten wire baskets to contain the individual sources, and layer thickness is controlled by evaporation to completion (Au: 1200-1600A°; Ni: 50-150A°). alloying is accomplished at an optimum established to be 525°C for two minutes. Contacts are processed using standard photolithography techniques. Pulse-plating of 1-3 microns of gold or silver to the base metallization pattern will be employed to assure sharp vertical plating features and to reduce unnecessary shadowing or overlap of metallization patterns.

P-contacts will be fabricated similarly to the n-contacts except gold-zinc alloy is used instead of Au/Ge/Ni or Au/Ni during the evaporation step. Stable contacts to semiconductor laser and LED GaP and GaAsP structures have become a well-controlled manufacturing science and we do not expect this area to be a problem.

EXPERIMENTAL RESULTS

The growth of smooth, uniform layers of $GaAs_xP_{1-x}$ on GaP substrates with x of the top layers ranging from 0.4 to 0.68 and energy gaps of 2.07 eV to 1.81 eV has been successfully demonstrated. These layers were grown using a combination of step grading and depletion grading.

A GaAsP structure has been designed which will allow the exploration of a range of energy band gaps between 1.75 eV and 2.07 eV for the top solar cell. The higher energy gaps may lead to improved "real" system performance in a four terminal configuration.

The solar cell structure is being grown using liquid phase epitaxial growth techniques. Three-layer structures grading from $GaAs_{.4}P_{.6}$ (2.07 eV) to $GaAs_{.68}P_{.32}$ (1.81 eV) have been produced in our laboratories using LPE.

The solar cell development to date has been most encouraging. The overall goal is to produce GaAsP top cell having Voc 1.50 volts, Jsc 17.8 mA/cm^2, a fill factor of 0.89, and an overall efficiency of 17.6%, based on the details shown in Table II. To date we have achieved a maximum Jsc of 10.6 mA/cm^2 (corrected for reflection losses), a maximum Voc of 1.394 volts and fill factors greater than 0.75. The present plan is to optimize each parameter separately using simplified col-

lector structures to optimize Voc, and Schottky and MIS structures to optimize, measure, and improve diffusion lengths and Jsc. Ohmic contacts for these structures, which are reproducible and reliable and have shown good mechanical adhesion in tests to date, have been developed.

CONCLUSIONS

Preliminary results are encouraging for the development of a wide band gap GaAsP top solar cell for attachment to conventional silicon solar cells. Solar conversion efficiency increases of over 50% may be expected with the successful development of this technology.

References:

[1] J. C. C. Fan, B.- Y. Tsaur, B. J. Palm, "Optical Design of High Efficiency Tandem Cells", Conf. Rec. 16th IEEE Photovoltaic Specialists Conference, p. 692, (1982).

[2] A. M. Barnett, M. G. Mauk, J. C. Zolper, I. W. Hall, W. A. Tiller, J. B. McNeely and R. B. Hall, "Thin Film Silicon and GaAs Solar Cells", Conf. Rec. 17th IEEE Photovoltaic Specialists Conf., 747, Orlando (1984).

[3] G. Sassi, "Theoretical Analysis of Solar Cells based on Graded Band-Gap Structures", J. Appl. Phys., 54, (9), 5421, (1983).

[4] L. R. Dawson, "Liquid Phase Epitaxy", Progress in Solid State Chemistry, Chapter 4, 7, 117, Pergamon Press (1972).

[5] R. L. Moon, "Liquid Phase Epitaxy" Chapter 11, Crystal Growth, ed. B. Pamplin, 2nd ed., p. 421, Pergamon Press, (1980).

[6] R. L. Moon, G. A. Antypas, Y. G. Chai, "Continuous Compositional Grading by LPE in Al-Ga-V Quaternary Alloys", Proceedings of the 7th International Symposium on GaAs and Related Compounds, p. 78, ed. C. M. Wolfe, Institute of Physics, London, (1978).

[7] S. Yamazaki, K. Nakajima, S. Komiya, Y. Kishi and K. Akita, "Liquid Phase Epitaxial Growth of InP/InGaAsP/InP Double-Heterostructure Wafers Free of Misfit dislocations", Appl. Phys. Lett. 43, (1), 82 (1983).

[8] H. Nelson, "Depositing Successive Layers from the Liquid Phase", U. S. Patent 3,565,702, February 23, 1971.

[9] H. J. Hovel and J. M. Woodall, "An Isothermal Etchback-Regrowth Method for High Efficiency $Ga_{1-x}Al_xAs$-GaAs Solar Cells", Appl. Phys. Lett., 30, 492 (1977).

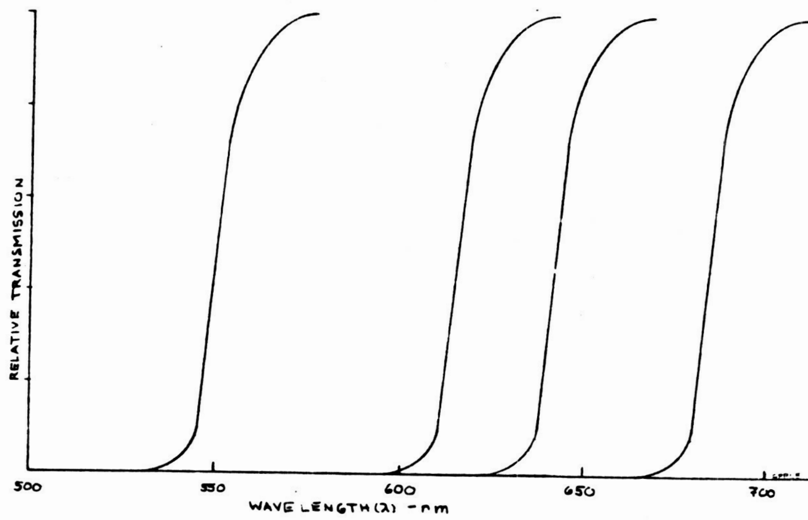

Figure 1. GaAsP on GaP Transmission Data

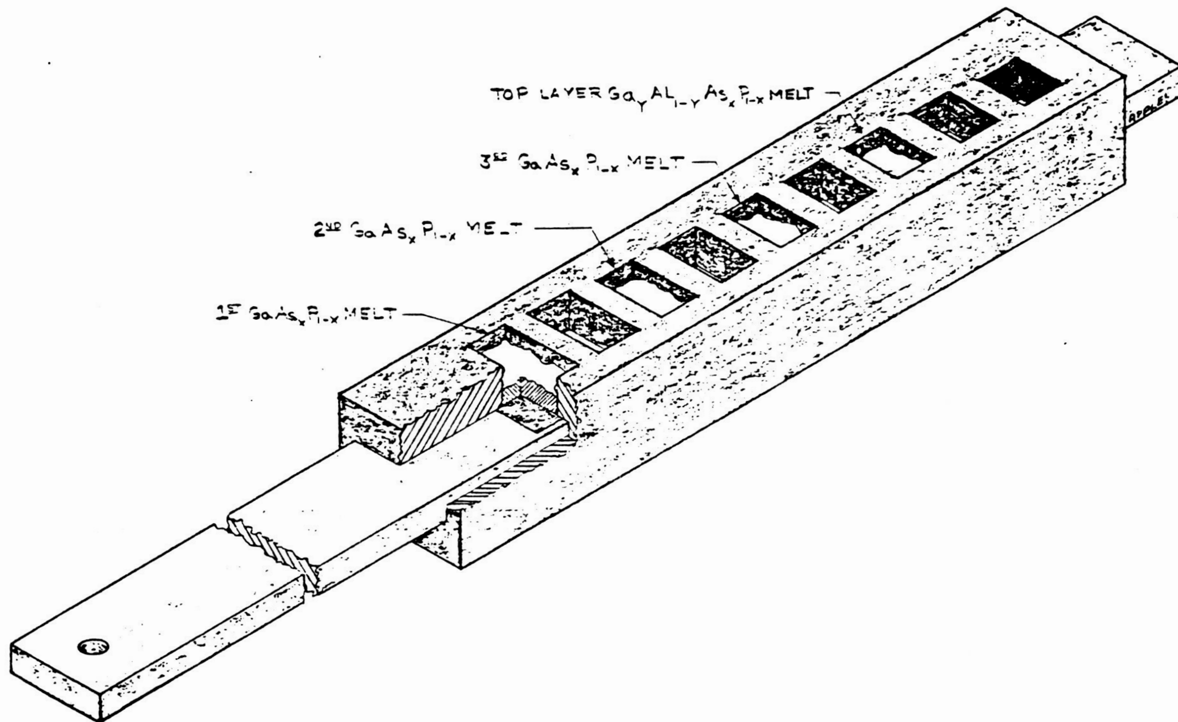

Figure 2. Slider boat growth apparatus showing the graded well width.

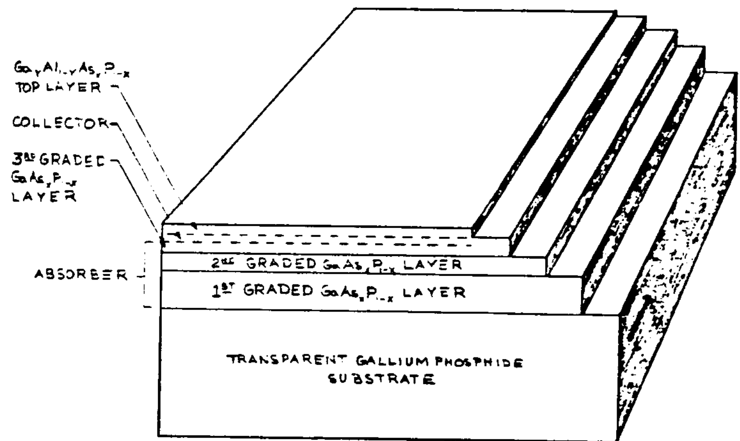

Figure 3. Multi-layer GaAsP on GaP solar cell structure (not to scale). Each successive layer is narrower than its predecessor, which allows easy access to areas of the individual growth surfaces for diagnostic purposes.

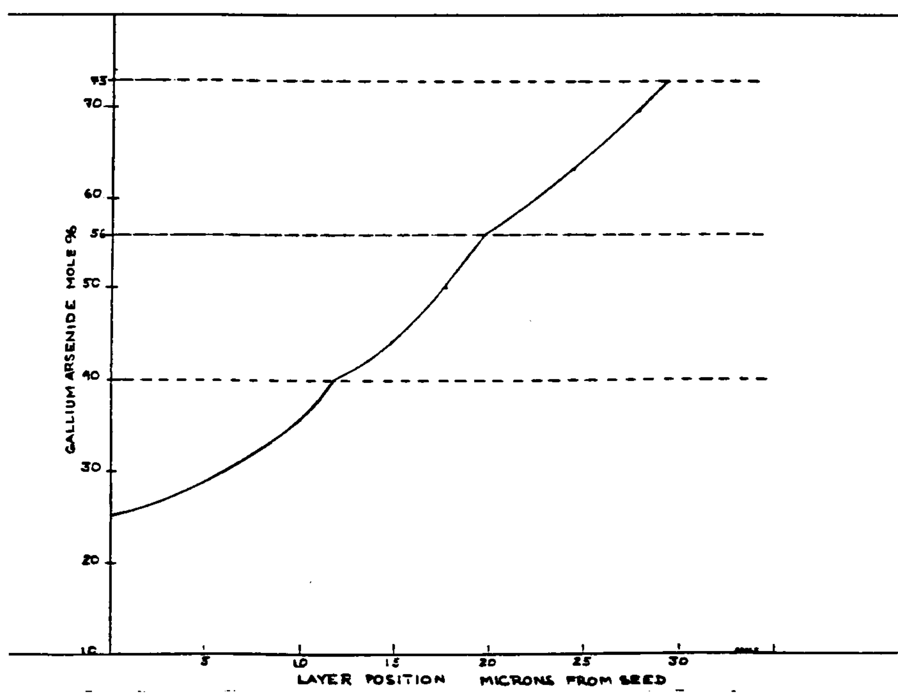

Figure 4. Compositional graded three-layer GaAsP on GaP Structure